

AN APPROACH TO NONLINEAR STATE ESTIMATION USING EXTENDED FIR FILTERING

°Shunyi Zhao, *Juan Pomárico-Franquiz, *Yuriy S. Shmaliy

°Key Laboratory of Advanced Process Control for Light Industry, Jiangnan University, Wuxi, P.R. China

*Department of Electronics Engineering, Universidad de Guanajuato, Salamanca, 36885, Mexico

ABSTRACT

A new technique called extended finite impulse response (EFIR) filtering is developed to nonlinear state estimation in discrete time state space. The EFIR filter belongs to a family of unbiased FIR filters which completely ignore the noise statistics. An optimal averaging horizon of N_{opt} points required by the EFIR filter can be determined via measurements with much smaller efforts and cost than for the noise statistics. These properties of EFIR filtering are distinctive advantages against the extended Kalman filter (EKF). A payment for this is an $N_{\text{opt}} - 1$ times longer operation which, however, can be reduced to that of the EKF by using parallel computing. Based on extensive simulations of diverse nonlinear models, we show that EFIR filtering is more successful in accuracy and more robust than EKF under the unknown noise statistics and model uncertainties.

1. INTRODUCTION

Nonlinear estimation problems arise in diverse fields of applications such as navigation, tracking, robotics, communications, control, etc. A traditional tool here is the extended Kalman filter (EKF) [1,2] having strong engineering features such as high accuracy, fast computation, easy coding, and small memory. However, EKF has several widely recognized flaws: 1) its estimate can be biased if noise is nonadditive, 2) it may diverge if nonlinearities and noise are large [3], and 3) its accuracy can be low if noise covariances are not well specified or ill-conditioned and noise is nonwhite Gaussian, heavy-tailed, or Gaussian with outliers [4].

Because it is desirable to have an estimator that is more robust than EKF, several other approaches were developed during decades [5–17]. The technique called the unscented transform was used in [12] to transfer the mean and variance through nonlinearities. A relevant filter called the unscented Kalman filter (UKF) has demonstrated better performance than EKF when the model is highly nonlinear. For continuous-time state-space models decomposed into “cells,” a grid-based method was worked out to approximate the posterior probability density function (pdf) of the process. The approach has resulted in the hidden Markov model (HMM) filters [13,14]. A sequential Monte Carlo (SMC) method also known as a particle filter (PF) [15] was developed to estimate Bayesian models associated with Markov chains in discrete-time domain. The reader can find a comprehensive review of these and other nonlinear filters in [16].

A novel alternative to the recursive EKF is the iterative extended finite impulse response (EFIR) filter [17, 18]. Unlike the EKF, UKF, and optimal FIR (OFIR) filters [19, 20], the EFIR filter totally ignores the noise statistics and initial error statistics. Similarly to PFs, the EFIR filter exploits most

recent past measurements which number is required to be optimal N_{opt} . A scalar N_{opt} can be determined by using test reference measurements or even via regular measurements without a reference signal [21], thus in a way much easier than that used to determine the noise statistics required by the Kalman filter. Finally, the EFIR filter belongs to a regression-based family of Gauss’s least squares estimators which are known to often give accuracy that is superior to the best available EKF [16]. Referring to such properties of EFIR filtering, one may expect new solutions to nonlinear estimation problems in different areas of applications. Thus, efficient EFIR algorithms are required to meet practical needs. Below, we consider a general nonlinear discrete-time state-space model, develop an iterative EFIR filtering algorithm, and learn its properties in a comparison with EKF based on two examples.

2. EXTENDED UNBIASED FIR FILTERING

In order to provide state estimation on a finite interval of N points, in this section we consider a general nonlinear discrete-time state-space model and develop an iterative EFIR algorithm.

2.1 Nonlinear State-Space Model

Consider a nonlinear process represented in state space with the state and observation equations,

$$\mathbf{x}_n = \mathbf{f}_n(\mathbf{x}_{n-1}, \mathbf{u}_n, \mathbf{w}_n, \mathbf{e}_n), \quad (1)$$

$$\mathbf{z}_n = \mathbf{h}_n(\mathbf{x}_n, \mathbf{v}_n), \quad (2)$$

in which $\mathbf{x}_n \in \mathbb{R}^K$ is the state vector, $\mathbf{u}_n \in \mathbb{R}^L$ is the input vector, $\mathbf{z}_n \in \mathbb{R}^M$ is the measurement vector, and $\mathbf{f}_n(\cdot)$ and $\mathbf{h}_n(\cdot)$ are nonlinear time-varying functions. We suppose that all random components are zero mean white Gaussian and uncorrelated. Namely, the process noise $\mathbf{w}_n \in \mathbb{R}^P$, the input noise $\mathbf{e}_n \in \mathbb{R}^H$, and the observation noise $\mathbf{v}_n \in \mathbb{R}^M$ have the properties: $E\{\mathbf{w}_n\} = \mathbf{0}$, $E\{\mathbf{e}_n\} = \mathbf{0}$, $E\{\mathbf{v}_n\} = \mathbf{0}$, and $E\{\mathbf{w}_i \mathbf{e}_j^T\} = \mathbf{0}$, $E\{\mathbf{w}_i \mathbf{v}_j^T\} = \mathbf{0}$, and $E\{\mathbf{v}_i \mathbf{e}_j^T\} = \mathbf{0}$ for all i and j . The noise covariances are depicted as $\mathbf{Q} = E\{\mathbf{w}_n \mathbf{w}_n^T\}$, $\mathbf{L} = E\{\mathbf{e}_n \mathbf{e}_n^T\}$, and $\mathbf{R} = E\{\mathbf{v}_n \mathbf{v}_n^T\}$.

To apply a technique such as Kalman filtering, both (1) and (2) need to be expanded to the 1-order or 2-order Taylor series [1, 2]. Aimed at demonstrating advantages of the FIR approach and referring to the fact that the 2-order expansion gives no definitive advantages [17, 22], below we employ only the 1-order expansions of $\mathbf{f}_n(\cdot)$ at $n-1$ and $\mathbf{h}_n(\cdot)$ at n under the following suppositions. We think that \mathbf{u}_n is slow enough and such that the difference $\mathbf{u}_n - \mathbf{u}_{n-1}$ is insignificant. We also allow the initial values to be known, to

Table 1: EKF Algorithm

Input: $\mathbf{z}_n, \hat{\mathbf{x}}_0, \mathbf{P}_0, \mathbf{R}, \mathbf{Q}, \mathbf{L}$
1: for $n = 1 : M$ do
2: $\hat{\mathbf{x}}_n^- = \mathbf{f}_n(\hat{\mathbf{x}}_{n-1}, \mathbf{u}_n, \mathbf{0}, \mathbf{0})$
3: $\mathbf{P}_n^- = \mathbf{F}_n \mathbf{P}_{n-1} \mathbf{F}_n^T + \mathbf{W}_n \mathbf{Q} \mathbf{W}_n^T + \mathbf{E}_n \mathbf{L} \mathbf{E}_n^T$
4: $\mathbf{K}_n = \mathbf{P}_n^- \mathbf{H}_n^T (\mathbf{H}_n \mathbf{P}_n^- \mathbf{H}_n^T + \mathbf{T}_n \mathbf{R}_n \mathbf{T}_n^T)^{-1}$
5: $\hat{\mathbf{x}}_n = \hat{\mathbf{x}}_n^- + \mathbf{K}_n [\mathbf{z}_n - \mathbf{h}_n(\hat{\mathbf{x}}_n^-, \mathbf{0})]$
6: $\mathbf{P}_n = (\mathbf{I} - \mathbf{K}_n \mathbf{H}_n) \mathbf{P}_n^-$
7: and for
Output: $\hat{\mathbf{x}}_n$

mean that the noise components at the start point are zeros. Accordingly, the expanded nonlinear functions become

$$\mathbf{f}_n = \mathbf{F}_n \mathbf{x}_{n-1} + \bar{\mathbf{u}}_n + \mathbf{W}_n \mathbf{w}_n + \mathbf{E}_n \mathbf{e}_n + \xi_n, \quad (3)$$

$$\mathbf{h}_n = \mathbf{H}_n \mathbf{x}_n + \bar{\mathbf{z}}_n + \mathbf{T}_n \mathbf{v}_n + \zeta_n, \quad (4)$$

where $\mathbf{F}_n = \left. \frac{\partial \mathbf{f}_n}{\partial \mathbf{x}} \right|_{\hat{\mathbf{x}}_{n-1}}$, $\mathbf{W}_n = \left. \frac{\partial \mathbf{f}_n}{\partial \mathbf{w}} \right|_{\hat{\mathbf{x}}_{n-1}}$, $\mathbf{E}_n = \left. \frac{\partial \mathbf{f}_n}{\partial \mathbf{e}} \right|_{\hat{\mathbf{x}}_n^-}$, $\mathbf{T}_n = \left. \frac{\partial \mathbf{h}_n}{\partial \mathbf{v}} \right|_{\hat{\mathbf{x}}_n^-}$, and $\mathbf{H}_n = \left. \frac{\partial \mathbf{h}_n}{\partial \mathbf{x}} \right|_{\hat{\mathbf{x}}_n^-}$ are Jacobian and both $\bar{\mathbf{u}}_n = \mathbf{f}_n(\hat{\mathbf{x}}_{n-1}, \mathbf{u}_n, \mathbf{0}, \mathbf{0}) - \mathbf{F}_n \hat{\mathbf{x}}_{n-1}$ and $\bar{\mathbf{z}}_n = \mathbf{h}_n(\hat{\mathbf{x}}_n^-) - \mathbf{H}_n \hat{\mathbf{x}}_n^-$ are known. Here, $\hat{\mathbf{x}}_n$ is the estimate¹ and $\hat{\mathbf{x}}_n^-$ is the prior estimate of \mathbf{x}_n . The residuals ξ_n and ζ_n are supposed to be small if the model is sufficiently smooth.

The 1-order expanded state-space model is thus

$$\mathbf{x}_n = \mathbf{F}_n \mathbf{x}_{n-1} + \bar{\mathbf{u}}_n + \tilde{\mathbf{e}}_n + \tilde{\mathbf{w}}_n + \xi_n, \quad (5)$$

$$\mathbf{z}_n = \mathbf{H}_n \mathbf{x}_n + \bar{\mathbf{z}}_n + \tilde{\mathbf{v}}_n + \zeta_n, \quad (6)$$

where the zero mean noise vectors $\tilde{\mathbf{w}}_n = \mathbf{W}_n \mathbf{w}_n$, $\tilde{\mathbf{e}}_n = \mathbf{E}_n \mathbf{e}_n$, and $\tilde{\mathbf{v}}_n = \mathbf{T}_n \mathbf{v}_n$ have the covariances $\tilde{\mathbf{Q}}_n = \mathbf{F}_n \mathbf{Q} \mathbf{F}_n^T$, $\tilde{\mathbf{L}}_n = \mathbf{E}_n \mathbf{L} \mathbf{E}_n^T$, and $\tilde{\mathbf{R}}_n = \mathbf{T}_n \mathbf{R} \mathbf{T}_n^T$, respectively.

Provided (5) and (6), the EKF can be coded as in Table 1, in which the initial state estimate $\hat{\mathbf{x}}_0$ and covariances \mathbf{P}_0 , \mathbf{R} , \mathbf{Q} , and \mathbf{L} are supposed to be known. The prior estimation error covariance matrix \mathbf{P}_n^- and estimation error covariance matrix \mathbf{P}_n are defined as

$$\mathbf{P}_n^- = E\{(\mathbf{x}_n - \hat{\mathbf{x}}_n^-)(\mathbf{x}_n - \hat{\mathbf{x}}_n^-)^T\}, \quad (7)$$

$$\mathbf{P}_n = E\{(\mathbf{x}_n - \hat{\mathbf{x}}_n)(\mathbf{x}_n - \hat{\mathbf{x}}_n)^T\}. \quad (8)$$

and we notice again that the required noise statistics \mathbf{P}_0 , \mathbf{R} , \mathbf{Q} , and \mathbf{L} are typically not well known to the engineer [4] that may cause unacceptable errors in EKF.

2.2 EFIR Filtering Algorithm

Unlike the recursive EKF, the iterative EFIR filter [17] utilizes measurements \mathbf{z}_n available on an interval of N past neighboring points from $m = n - N + 1$ to n . The EFIR filter totally ignores the covariances \mathbf{R} , \mathbf{Q} , \mathbf{L} , and \mathbf{P}_0 . Instead, it requires an optimal averaging interval of N_{opt} points in order to minimize the mean square error. There are two simple ways to find N_{opt} :

¹ $\hat{\mathbf{x}}_{n|k}$ means the estimate at n via measurement from the past to k . Below, we use the following notations: $\hat{\mathbf{x}}_n \triangleq \hat{\mathbf{x}}_{n|n}$ and $\hat{\mathbf{x}}_n^- \triangleq \hat{\mathbf{x}}_{n|n-1}$.

- Via test measurements implying a known model \mathbf{x}_n by minimizing the trace of \mathbf{P}_n ,

$$N_{\text{opt}} = \arg \min_N \{\text{tr} \mathbf{P}(N)\}. \quad (9)$$

- Utilizing measurements with no reference signal as shown in [21].

The EFIR filtering estimate has the Kalman form

$$\hat{\mathbf{x}}_l = \hat{\mathbf{x}}_l^- + \mathbf{K}_l [\mathbf{z}_l - \mathbf{h}_l(\hat{\mathbf{x}}_l^-)], \quad (10)$$

in which an iterative variable l ranges from $m + K$ to n , where K is the number of the states. For each time index n , the output is taken when $l = n$. The bias correction gain

$$\mathbf{K}_l = \mathbf{G}_l \mathbf{H}_l^T \quad (11)$$

is defined and updated iteratively via the generalized noise power gain (GNPG)

$$\mathbf{G}_l = [\mathbf{H}_l^T \mathbf{H}_l + (\mathbf{F}_l \mathbf{G}_{l-1} \mathbf{F}_l^T)^{-1}]^{-1}. \quad (12)$$

To avoid singularities, iterative computation of (10) starts at $m + K$ and all values at $s = m + K - 1$ are computed in short batch forms as [24]

$$\hat{\mathbf{x}}_s = \mathbf{F}_s \dots \mathbf{F}_{m+1} \Lambda_{s,m} \mathbf{H}_{s,m}^T \mathbf{Y}_{s,m}, \quad (13)$$

$$\mathbf{G}_s = \mathbf{F}_s \dots \mathbf{F}_{m+1} \Lambda_{s,m} \mathbf{F}_{m+1}^T \dots \mathbf{F}_s^T, \quad (14)$$

where $\Lambda_{s,m} = (\mathbf{H}_{s,m}^T \mathbf{H}_{s,m})^{-1}$ and

$$\mathbf{Y}_{s,m} = [\mathbf{y}_s^T \dots \mathbf{y}_{m+1}^T \mathbf{y}_m^T]^T, \quad (15)$$

$$\mathbf{H}_{s,m} = \begin{bmatrix} \mathbf{H}_s \mathbf{F}_s \dots \mathbf{F}_{m+1} \\ \vdots \\ \mathbf{H}_{m+1} \mathbf{F}_{m+1} \\ \mathbf{H}_m \end{bmatrix}. \quad (16)$$

Unlike the EKF relying on $\hat{\mathbf{x}}_0$, the EFIR filter needs N_{opt} known initial estimates or linear measurements united in a vector \mathbf{y}_n . Since \mathbf{y}_n may be unavailable in nonlinear modelling, the following options can be considered:

- If \mathbf{y}_n is available, then compute $\hat{\mathbf{x}}_s$ via (13) using (15) and (16) and set $\mathbf{y}_s = \hat{\mathbf{x}}_s$.
- If \mathbf{y}_n is unavailable, then the output of EKF or some other estimator (even rough) can be used as \mathbf{y}_s . Otherwise, if all of the states are observable by \mathbf{z}_n , a solution to $\mathbf{z}_n = \mathbf{h}_n(\mathbf{x}_n, \mathbf{0})$ for \mathbf{x}_n can be employed as \mathbf{y}_n [17].
- If (2) is linear, then set $\mathbf{y}_n = \mathbf{z}_n$.

Based upon the results obtained in [17] and following the above-given notations, an iterative EFIR filter associated with (5) and (6) can be coded as in Table 2. Provided \mathbf{z}_n and \mathbf{y}_n , it needs only N and K to start computing and updating all the vectors and matrices. No noise statistics are involved. Herewith, there are two specifics which should be taken into account by the users:

- Because GNPG is almost unity on an interval of K points, \mathbf{G}_s in many cases can be substituted with an identity matrix \mathbf{I} .
- The EFIR algorithm operates in $N_{\text{opt}} - 1$ times slower than EKF owing to iterations. Therefore, its implementation based on parallel computing may be preferable.

Table 2: EFIR Filtering Algorithm

Input: z_n, y_n, K, N	
1:	for $n = N - 1 : M$ do
2:	$m = n - N + 1, \quad s = m + K - 1$
3:	$\tilde{\mathbf{x}}_s = \begin{cases} \mathbf{y}_s, & \text{if } s < N - 1 \\ \hat{\mathbf{x}}_s, & \text{if } s \geq N - 1 \end{cases}$
4:	$\mathbf{G}_s = \mathbf{F}_s \dots \mathbf{F}_{m+1} (\mathbf{H}_{s,m}^T \mathbf{H}_{s,m})^{-1} \mathbf{F}_{m+1}^T \dots \mathbf{F}_s^T$
5:	for $l = m + K : n$ do
6:	$\tilde{\mathbf{x}}_l^- = \mathbf{f}_l(\tilde{\mathbf{x}}_{l-1}, \mathbf{u}_l, \mathbf{0}, \mathbf{0})$
7:	$\mathbf{G}_l = [\mathbf{H}_l^T \mathbf{H}_l + (\mathbf{F}_l \mathbf{G}_{l-1} \mathbf{F}_l^T)^{-1}]^{-1}$
8:	$\mathbf{K}_l = \mathbf{G}_l \mathbf{H}_l^T$
9:	$\tilde{\mathbf{x}}_l = \tilde{\mathbf{x}}_l^- + \mathbf{K}_l [z_l - \mathbf{h}_l(\tilde{\mathbf{x}}_l^-)]$
10:	and for
11:	$\hat{\mathbf{x}}_n = \tilde{\mathbf{x}}_n$
12:	and for
Output: $\hat{\mathbf{x}}_n$	

3. APPLICATIONS

As examples of applications, we first consider indoor robot localization provided using radio frequency identification (RFID) tags. We then consider tracking of a moving object with temporary model uncertainties.

3.1 Robot Localization

A robot travels in direction d with coordinates x_n and y_n on an indoor floorspace. It measures distances to two RFID tags, A and B, and its trajectory is controlled by the left and right wheels. The distance between the wheels is $b = 1$ m and the incremental distances vehicle travels by these wheels are d_L and d_R . The pose angle Φ_n is measured with an imbedded fiber optic gyroscope (FOG) [23].

The robot expanded state-space model is (5) and (6) in which $\mathbf{x}_n = [x_n \ y_n \ \Phi_n]^T$, $\mathbf{u}_n = [d_{Ln} \ d_{Rn}]^T$, $\mathbf{w}_n = [w_{xn} \ w_{yn} \ w_{\Phi n}]^T$, $\mathbf{e}_n = [e_{Ln} \ e_{Rn}]^T$, $\mathbf{T}_n = \mathbf{I}$, $\mathbf{W}_n = \mathbf{F}_n$,

$$\mathbf{F}_n = \begin{bmatrix} 1 & 0 & -d_n \sin(\hat{\Phi}_{n-1} + \frac{1}{2}\phi_n) \\ 0 & 1 & d_n \cos(\hat{\Phi}_{n-1} + \frac{1}{2}\phi_n) \\ 0 & 0 & 1 \end{bmatrix}, \quad (17)$$

$$\mathbf{E}_n = \frac{1}{2b} \begin{bmatrix} be_{cn} + d_n e_{sn} & be_{cn} - d_n e_{sn} \\ be_{sn} - d_n e_{cn} & be_{sn} + d_n e_{cn} \\ -2 & 2 \end{bmatrix}, \quad (18)$$

$$\mathbf{H}_n = \begin{bmatrix} \frac{\hat{x}_n^- - x_1}{u_{1n}} & \frac{\hat{y}_n^- - y_1}{u_{1n}} & 0 \\ \frac{\hat{x}_n^- - x_2}{u_{2n}} & \frac{\hat{y}_n^- - y_2}{u_{2n}} & 0 \\ 0 & 0 & 1 \end{bmatrix}, \quad (19)$$

where $u_{1n} = \sqrt{(y_1 - \hat{y}_n^-)^2 + (x_1 - \hat{x}_n^-)^2 + c_1^2}$, $u_{2n} = \sqrt{(y_2 - \hat{y}_n^-)^2 + (x_2 - \hat{x}_n^-)^2 + c_2^2}$, $d_n = \frac{1}{2}(d_{Rn} + d_{Ln})$, $\phi_n \cong \frac{1}{b}(d_{Rn} - d_{Ln})$, $e_{cn} = \cos(\hat{\Phi}_n^- + \frac{\phi_n}{2})$, and $e_{sn} = \sin(\hat{\Phi}_n^- + \frac{\phi_n}{2})$. We allow all the covariance ma-

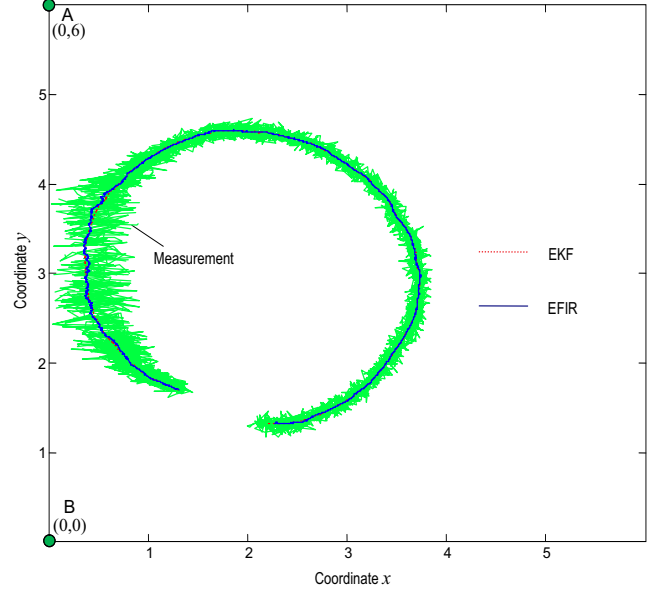


Figure 1: Measurements and EKF and EFIR filtering estimates of robot location within the ranges of two RFID tags, A and B, in the ideal case of fully known noise statistics and $N_{\text{opt}} = 74$.

trices to be diagonal and set the standard deviations $\sigma_x = \sigma_y = \sigma_L = \sigma_R = 1$ mm, $\sigma_\Phi = 0.5^\circ$, $\sigma_{v1} = \sigma_{v2} = 5$ sm, and $\sigma_{v3} = 2^\circ$. The reader range is supposed to be $r = 6$ m. We place a tag A at $(0, 6)$ m and tag B at $(0, 0)$ m and let $d_L = 0.12$ mm and $d_R = 0.24$ mm. Simulation is provided at 5000 points with time interval T allowing $\mathbf{G}_s = \mathbf{I}$.

Since direct measurements of x_n and y_n are unavailable, we solve the inverse problem in (6) for $x_1 = x_2 = y_2 = 0$ and $y_1 = 6$ m, and provide “linear” measurements \tilde{x}_n and \tilde{y}_n of x_n and y_n united in a measurement vector $\mathbf{y}_n = [\tilde{x}_n \ \tilde{y}_n]^T$. Typical measurements \tilde{x}_n and \tilde{y}_n along with the EKF and EFIR estimates are shown in Fig. 1 for exactly known noise covariances \mathbf{R} , \mathbf{Q} , and \mathbf{L} , initial state $\hat{\mathbf{x}}_0 = \mathbf{y}_0$, and initial error $\mathbf{P}_0 = \mathbf{0}$.

By test measurements, we obtain the model \mathbf{x}_n and find $N_{\text{opt}} = 74$ by minimizing the trace of \mathbf{P}_n via (9) as shown in Fig. 2a. Under such conditions, the estimates sketched in Fig. 1 can be considered as the best available by the EFIR filter and EKF. It is seen that the estimates are consistent, although both filters produce larger errors close to the boundary linking the tags.

Because an ideal situation is unfeasible, we next learn effect of errors in the noise covariances on EKF estimates. In doing so, we introduce a correction coefficient p to the covariance matrices as $p^2 \mathbf{R}$, \mathbf{Q}/p^2 , and \mathbf{L}/p^2 and compute the trace of $\mathbf{P}(p)$ using (8) for EKF as shown in Fig. 2b. Here, we also depict the p -invariant trace of \mathbf{P} for the EFIR filter ($N_{\text{opt}} = 74$). As expected, the EKF is a bit more accurate than EFIR filter in the ideal case of $p = 1$. However, that is only when $0.6 < p < 2$ that EKF outperforms the EFIR filter with an insignificant difference of about 0.5 mm. Otherwise, the EFIR filter is more accurate. Since a scalar N_{opt} can be found in a way much easier than that required for \mathbf{R} , \mathbf{Q} , and \mathbf{L} , we consider it as a distinctive advantage of the EFIR filter. Note that, for the sake of correctness, the covariance matrices must first be specified in continuous time and then converted to discrete time that requires additional mathematical efforts.

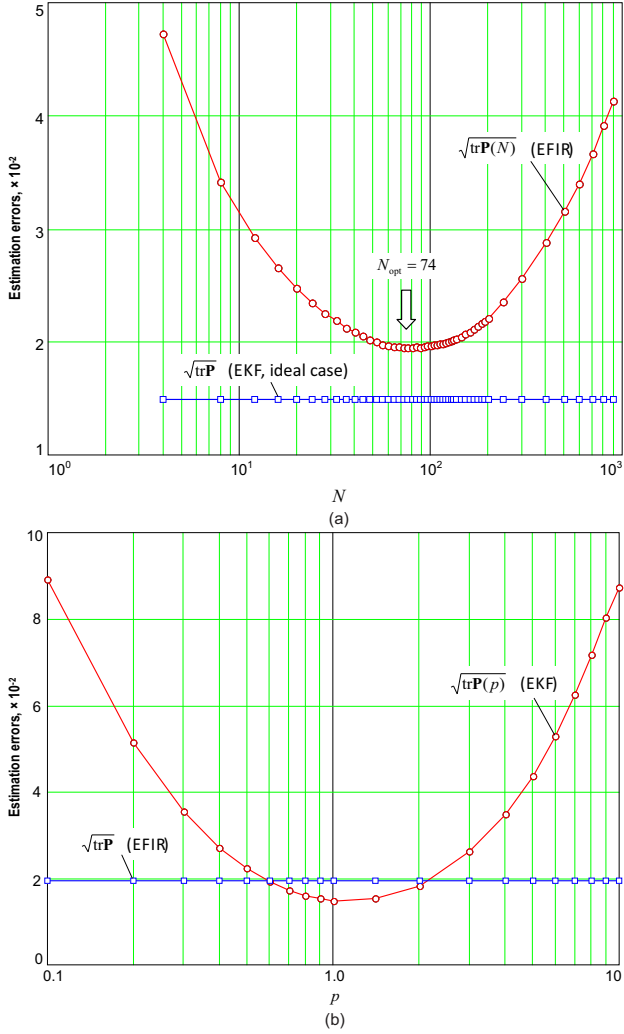


Figure 2: Errors of EKF and EFIR filtering corresponding to Fig. 1: (a) $\sqrt{\text{tr}\mathbf{P}(N)}$ of EFIR filter and $\sqrt{\text{tr}\mathbf{P}}$ of EKF and (b) $\sqrt{\text{tr}\mathbf{P}(p)}$ of EFIR filter and $\sqrt{\text{tr}\mathbf{P}(p)}$ of EKF.

Moreover, cost measurements are commonly required to determine \mathbf{R} , \mathbf{Q} , and \mathbf{L} .

Practical experience shows that errors in the determination of \mathbf{R} , \mathbf{Q} , and \mathbf{L} can be large [4]. On the other hand, N_{opt} can be found accurately even without a reference signal [21]. We therefore admit $p = 5$ and $N_{\text{opt}} = 74$ and take a more precise look at possible estimation errors $\varepsilon_n = \mathbf{x}_n - \hat{\mathbf{x}}_n$ in the time domain. Typical results sketched in Fig. 3 reveal larger “slow” noise in all EKF estimates. In an opposite case of $p < 0.5$, all EKF estimates are accompanied with larger “fast” noise. Moreover, the EKF has appeared to be strongly addicted to divergence when $p < 0.5$. This fact still unknown in nonlinear filtering may help viewing the Kalman divergence from the other side. Returning back to Fig. 1, we finally notice that in the ideal case of $p = 1$ the EKF and EFIR estimates do not get away essentially from each other and are almost indistinguishable.

3.2 Tracking with Temporary Model Uncertainties

We now consider a typical problem when two distance measurement stations (DMSs) are located at $(0, 0)$ and $(0, a =$

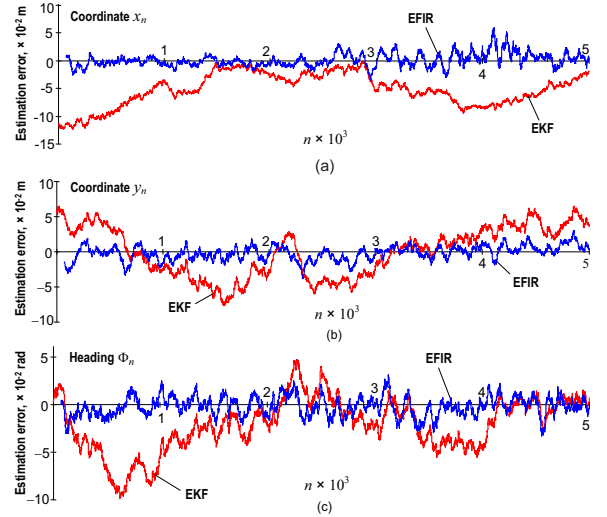


Figure 3: Typical time-domain errors of EKF and EFIR filtering corresponding to Fig. 1 for $p = 5$ and $N_{\text{opt}} = 74$: (a) coordinate x , (b) coordinate y , and (c) heading Φ .

50 m) and that a moving object and DMSs are in a horizontal plane. Each DMS transmits a pulse that is reflected from the object and returns back to DMS. The transit time is interpreted in terms of distance d_1 or d_2 .

We suppose that an object moves in the presence of noise along each of the axes and has four states ($K = 4$): x_{1n} is the coordinate x ; x_{2n} velocity along x ; $x_{3n} \geq 0$ coordinate y ; and x_{4n} velocity along y . The behavior is modeled with equations

$$\mathbf{x}_n = \mathbf{A}\mathbf{x}_{n-1} + \mathbf{w}_n, \quad (20)$$

$$\mathbf{y}_n = \mathbf{h}_n(\mathbf{x}_n) + \mathbf{v}_n, \quad (21)$$

in which $\mathbf{x}_n = [x_{1n} x_{2n} x_{3n} x_{4n}]^T$ and

$$\mathbf{A} = \begin{bmatrix} 1 & \tau + \delta_n & 0 & 0 \\ 0 & 1 & 0 & 0 \\ 0 & 0 & 1 & \tau + \delta_n \\ 0 & 0 & 0 & 1 \end{bmatrix}, \quad (22)$$

where $\delta_n \neq 0$ if $400 \leq n \leq 440$ and is zero otherwise. To gain the effect, we set $\delta_n = 10 \text{ s} \gg \tau = 0.1 \text{ s}$. It is supposed that white Gaussian noise $\mathbf{w}_n = [0 \ w_{2n} \ 0 \ w_{4n}]^T$ is zero mean with the variances $\sigma_w^2 = \sigma_{w2}^2 = \sigma_{w4}^2$ and

$$\mathbf{R} = \sigma_w^2 \begin{bmatrix} \tau^2/3 & \tau/2 & 0 & 0 \\ \tau/2 & 1 & 0 & 0 \\ 0 & 0 & \tau^2/3 & \tau/2 \\ 0 & 0 & \tau/2 & 1 \end{bmatrix}. \quad (23)$$

In such a model we have

$$\mathbf{h}_n(\mathbf{x}_n) = \begin{bmatrix} \sqrt{x_n^2 + y_n^2} \\ \sqrt{(a - x_n)^2 + y_n^2} \end{bmatrix} \quad (24)$$

and allow noise $\mathbf{v}_n = [v_{1n} \ v_{2n}]$ to have the variance $\sigma_v^2 = \sigma_{v1}^2 = \sigma_{v2}^2$ and covariance

$$\mathbf{Q} = \begin{bmatrix} \sigma_v^2 & 0 \\ 0 & \sigma_v^2 \end{bmatrix}. \quad (25)$$

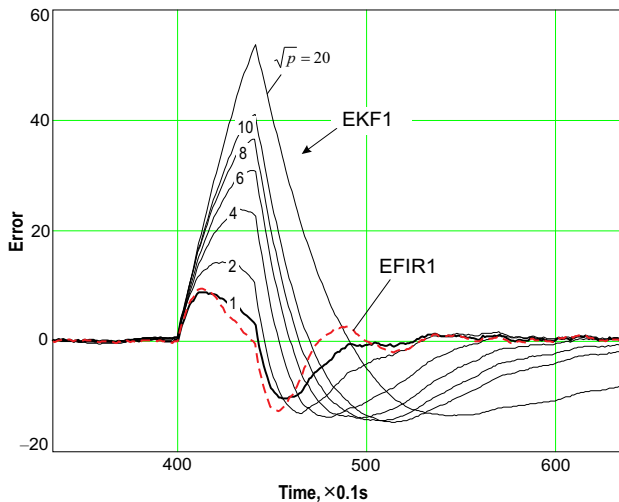


Figure 4: Effect of the temporary model uncertainty occurred from $n = 400$ to $n = 440$ on the estimation errors with $p \geq 1$.

Simulation has been conducted at 1000 points with step $\tau = 0.1$ s for $\sigma_w = 0.01$ m and $\sigma_v = 0.2$ m. The result shown in Fig. 4 confirms a statement made in [24] for linear filtering: EKF is much lesser robust against the temporary model uncertainties in the presence of errors in noise covariances.

4. CONCLUSIONS

In this paper, we have developed and studied an efficient iterative EFIR filtering algorithm. We have also shown several important advantages of this algorithm against the recursive EKF. It is only within a narrow range around the ideal conditions that EKF has better accuracy than EFIR. Otherwise, errors in EKF grow rapidly and may cause divergence, whereas the EFIR filter ignoring noise statistics remains at the same error level. Of practical importance is that the only tuning scalar value N_{opt} required by the EFIR filter can easily be specialized via test measurements or even using regular measurements with no reference. Moreover, the determination of N_{opt} requires much smaller efforts and cost than for the noise statistics, especially if the process is time-varying. A payment for this is an $N_{\text{opt}} - 1$ times longer operation required by the EFIR algorithm to complete iterations. This drawback can be circumvented using parallel computing.

REFERENCES

- [1] H. Cox, "On the estimation of state variables and parameters for noisy dynamic systems," *IEEE Trans. Automat. Contr.*, vol. 9, pp. 5–12, Jan. 1964.
- [2] M. Athans, R. P. Wishner, and A. Bertolini, "Suboptimal state estimation for continuous-time nonlinear systems from discrete noisy measurements," *IEEE Trans. Automat. Contr.*, vol. 13, pp. 504–514, Oct. 1968.
- [3] R. J. Fitzgerald, "Divergence of the Kalman filter," *IEEE Trans. Autom. Contr.*, vol. 16, pp. 736–747, Dec. 1971.
- [4] B. Gibbs, *Advanced Kalman Filtering, Least-Squares and Modeling*, New York: Wiley, 2011.
- [5] A. H. Jazwinski, *Stochastic Processes and Filtering Theory*, New York: Academic Press, 1970.
- [6] H. W. Sorenson, "On the development of practical nonlinear filters," *Information Science*, vol. 7, pp. 253–270, 1974.
- [7] F. E. Daum, "Exact finite dimensional nonlinear filters," *IEEE Trans. Autom. Contr.*, vol. 31, pp. 616–622, Jul. 1986.
- [8] G. J. Gordon, D. J. Salmond, and A. F. M. Smith, "Novel approach to nonlinear/non-Gaussian Bayesian state estimation," *IEE Proc. Radar Signal Process.*, pt. F, vol. 140, pp. 107–113, Apr. 1993.
- [9] H. Tanizaki, *Nonlinear Filters*, (2nd ed.), New York: Springer-Verlag, 1996.
- [10] S. Challa and Y. Bar-Shalom, "Nonlinear filter design using Fokker-Planck-Kolmogorov probability density evolutions," *IEEE Trans. Aerospace Electron. Syst.*, vol. 36, pp. 309–315, Jan. 2000.
- [11] K. Kastella and C. Kreucher, "Multiple model nonlinear filtering for low signal ground target applications," *IEEE Trans. Aerospace Electron. Syst.*, vol. 41, pp. 549–564, Apr. 2005.
- [12] S. J. Julier and J. K. Uhlmann, "A new extension of the Kalman filter to nonlinear systems," in: *Proc. SPIE*, vol. 3068, pp. 182–193, 1997.
- [13] F. Martinerie and P. Forster, "Data association and tracking using hidden Markov models and dynamic programming," in: *Proc. IEEE Int. Conf. Acoust. Speech Signal Process. (ICASSP-92)*, San Francisco, CA, 1992, pp. 449–452.
- [14] L. R. Rabiner and B. H. Juang, "An introduction to hidden Markov models," *IEEE Acoust. Speech Signal Process. Mag.*, vol. 3, pp. 4–16, Jan. 1986.
- [15] M. S. Arulampalam, S. Maskell, N. Gordon, and T. Clapp, "A tutorial on particle filters for online nonlinear/non-Gaussian Bayesian tracking," *IEEE Trans. Signal Process.*, vol. 50, pp. 174–188, Feb. 2002.
- [16] F. Daum, "Nonlinear filters: beyond the Kalman filter," *IEEE Aerospace & Electron. Systems Mag.*, vol. 20, pp. 57–69, Aug. 2005.
- [17] Y. S. Shmaliy, "Suboptimal FIR filtering of nonlinear models in additive white Gaussian noise," *IEEE Trans. Signal Process.*, vol. 60, pp. 5519–5527, Oct. 2012.
- [18] J. Pomrico-Franquiz, S. H. Khan, and Y. S. Shmaliy, "Combined extended FIR/Kalman filtering for indoor robot localization via triangulation", *Measurement*, vol. 50, pp. 236–243, Apr. 2014.
- [19] W. H. Kwon and S. Han, *Receding Horizon Control: Model Predictive Control for State Models*, London: Springer, 2005.
- [20] Y. S. Shmaliy, "Linear optimal FIR estimation of discrete time-invariant state-space models," *IEEE Trans. Signal Process.*, vol. 58, pp. 3086–3096, Jun. 2010.
- [21] F. Ramirez-Echeverria, A. Sarr, and Y. S. Shmaliy, "Optimal memory for discrete-time FIR filters in state space," *IEEE Trans. Signal Process.*, vol. 62, pp. 557–561, Feb. 2014.
- [22] D. Simon, *Optimal State Estimation*, Hoboken, NJ: Wiley, 2006.
- [23] K. Komoriya and E. Oyama, "Position estimation of a mobile robot using optical fiber gyroscope," in *Proc. IEEE/RSJ/CI Int. Conf. Intell. Robots Syst.*, vol. 1, pp. 143–149, 1994.
- [24] Y. S. Shmaliy, "An iterative Kalman-like algorithm ignoring noise and initial conditions," *IEEE Trans. Signal Process.*, vol. 59, pp. 2465–2473, Jun. 2011.